

Structural Intergrowth Phenomena in the Sb_xWO_3 System

T. EKSTRÖM,* M. PARMENTIER†‡ AND R. J. D. TILLEY†

* *Department of Inorganic Chemistry, Arrhenius Laboratory, University of Stockholm, S-106 91 Stockholm, Sweden, and † School of Materials Science, University of Bradford, Bradford BD7 1DP, West Yorkshire, England*

Received September 17, 1979; in revised form November 28, 1979

The Sb_xWO_3 system has been examined by powder X-ray diffraction and high-resolution electron microscopy. In the composition range $Sb_{0.01}WO_3$ and $Sb_{0.07}WO_3$, a series of perovskite-related tungsten bronzes form. In the composition range approximately $Sb_{0.12}WO_3$ to $Sb_{0.20}WO_3$, a series of structures were found which can be regarded as more or less ordered intergrowths of lamellae of the WO_3 and hexagonal tungsten bronze structures. The WO_3 slabs are n octahedra thick and a knowledge of the value of n allows the chemical composition of the phases, $x = 1/(2n + 1)$, to be calculated. No n values below 2 were observed and for $x > 0.15$, fairly large regions with the ordered $n = 2$ structure were found.

Introduction

In a previous article, it was reported that the direct reaction of antimony powder on tungsten trioxide at 1173 K resulted in a series of Sb_xWO_3 bronzes (1). At x values < 0.07 these bronzes were of the perovskite type, where the antimony metal atoms are interpolated in the cages between the WO_6 octahedra in the parent WO_3 structure. Similar perovskite bronzes have also been found to form for the other group VB metals arsenic and bismuth (2). In addition, another structure type was observed to be present in the Sb_xWO_3 system for x values > 0.07 . This phase apparently seemed to form alone at a composition of about $Sb_{0.15}WO_3$. In samples with still higher anti-

mony contents the presence of metallic antimony could be seen. In this respect the Sb_xWO_3 system differs from the As_xWO_3 and Bi_xWO_3 systems, where the perovskite bronze phases were the only ternary phases observed.

In an attempt to solve the crystal structure of the $Sb_{0.15}WO_3$ phase, single-crystal diffraction patterns were recorded using the Weissenberg technique and the intensity data obtained were evaluated by the Patterson method. As a result, a heavy-atom model was quite readily obtained from about 800 X-ray reflections, but the related reliability factor R was as high as 0.20. Further refinement of the structural model failed and the reason for this was not clearly understood at that time. The real positions of the Sb atoms in the structure were also open for discussion, as two distribution models could be postulated. Either a bronze-like structure could form in which

‡ On leave from: Laboratoire de Chimie Minérale-LA 158, University de Nancy 1 GO. 140, S4037 Nancy, Cedex, France.

the Sb atoms were inserted in a framework of corner-sharing WO_6 octahedra, or else a substitution of antimony for tungsten in the MO_6 octahedra could take place. In the latter case, however, this must be compensated for by a corresponding oxygen reduction, possibly by edge sharing between octahedra. This behavior has been observed in the Ti_xWO_3 system, where crystallographic shear (CS) planes are known to form (3).

In order to clarify these aspects we found it worthwhile to reinvestigate the Sb_xWO_3 system, especially for x values > 0.07 , using high-resolution electron microscopy besides X-ray methods. The results of this study are reported below and discussed in terms of the known crystal chemistry of the binary and ternary tungsten oxides.

Experimental

Most of the Sb_xWO_3 preparations were made by heating together Sb metal (Johnson Matthey) and WO_3 (Merck p.a.) in evacuated sealed silica ampoules. The temperatures employed were within the interval 1173 to 1473 K and the heating times used were from 12 hr to 4 weeks. An additional series of Sb_xWO_3 samples were prepared from mixtures of Sb_2O_3 (Baker's Analysed) WO_3 and WO_2 . The WO_3 for these experiments was obtained by thermal decomposition of H_2WO_4 (Matheson, Coleman and Bell) in air at 1073 K. WO_2 was obtained by reduction of the WO_3 in a stream of $\text{H}_2/\text{H}_2\text{O}$ gas mixture. These samples were heated for times ranging from 7 to 60 days at 1173 K. Also some samples were prepared at other gross compositions to clarify some aspects of the phase diagram in the region close to WO_3 . After the heat treatment, the samples were quickly removed from the furnace, but no particular precautions were taken to quench them especially rapidly.

All samples were thereafter examined by

recording their powder X-ray patterns at room temperature in a Guinier camera, using strictly monochromatic $\text{CuK}\alpha_1$ radiation and KCl ($a = 0.6292$ nm) or NaCl ($a = 0.5639$ nm) as an internal standard. In addition, most samples were studied optically by using a Zeiss Ultraphot microscope and selected samples were studied by transmission electron microscopy, using a JEM 100B electron microscope operated at 100 kV and fitted with a goniometer stage. The electron microscope specimens were prepared by crushing crystals in *n*-butanol in an agate mortar. A drop of the resulting suspension was allowed to dry on a net-like carbon film (4). Only fragments which projected over holes in the film were examined in detail.

Results

The results obtained from the varying techniques were in good agreement with one another and allowed the partial phase diagrams shown in Figs. 1a and b to be constructed. The results obtained are also in agreement with the previous data on the Sb_xWO_3 system (1). The two principal phase regions along the Sb_xWO_3 line in the

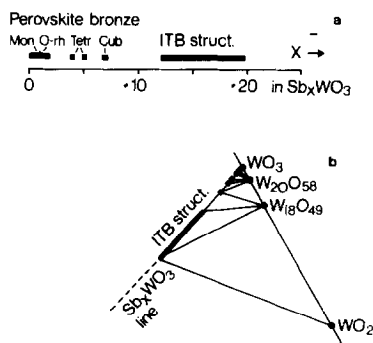


FIG. 1. (a) Phases present along the Sb_xWO_3 line of the Sb-W-O ternary system. (b) Phase relations in the Sb-W-O ternary system close to WO_3 , for preparations at 1173 K. In both diagrams ITB struct. stands for intergrowth bronze structures as described in the text.

phase diagram are described in more detail in the sections which follow.

Perovskite Related Bronzes

The results obtained in the Sb_xWO_3 system for $x < 0.1$ were straightforward and are shown in Fig. 1a. No significant differences could be observed by using antimony metal or antimony oxide as a starting material for the preparations. It was also found that varying the heating temperatures in the range 1173–1573 K caused no shifts in the observed phase limits, as seen at room temperature, for the perovskite bronzes which formed.

The symmetry of the Sb_xWO_3 bronze structure increased as the antimony content increased from monoclinic, through orthorhombic and tetragonal to cubic. The cubic bronze had the composition $Sb_{0.07}WO_3$, which was thus the highest antimony content observed in the series of perovskite-related bronzes. The shifts in the unit cell parameters for these bronzes are illustrated in Fig. 2 as a function of antimony content. Studies of the perovskite bronzes by electron microscopy showed

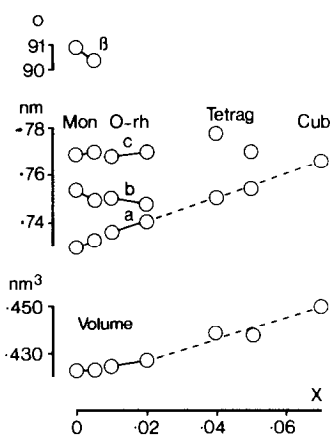


Fig. 2. Room temperature unit-cell parameters versus composition x for the bronzes Sb_xWO_3 . In the figure, the parameters $a = 2^{1/2}a_T$ and $c = 2c_T$ have been plotted for the tetragonal phase, where a_T and c_T are the crystallographic unit-cell parameters. Similarly, for the cubic form, $a = 2a_c$ has been used.

that no CS planes or other extended defects were present in the WO_3 -like structure.

Intergrowth Bronzes

The powder X-ray results for samples with $x > 0.07$ showed the presence of another phase in addition to the cubic perovskite bronze. When the gross composition of the samples reached $x = 0.15$ no additional lines of the cubic bronze could be seen in the patterns and at this composition the new material was apparently monophasic. The homogeneity range of the compound seemed to be extended to about $x = 0.20$, although quite often traces of unreacted antimony metal were observed in the preparations. No significant lattice parameter changes were observed for the phase as the overall composition of the samples varied within this region and it was possible to index the X-ray powder patterns using the parameters given earlier for this structure, namely, $a = 1.480$ nm, $b = 2.037$ nm, and $c = 1.515$ nm for the orthorhombic cell (1).

The electron microscope results were helpful in revealing the true nature of the phase region. It was found that in the composition range $0.12 < x < 0.20$, the samples contained mixed crystals containing structural intergrowth. Two structure types were intergrown in parallel slabs, lying in various sequences and to some extent without any evident order. This was especially true for lower x values, whereas for $x > 0.15$ fairly large regions within the crystals of an ordered intergrowth structure was found. Typical medium- and high-magnification micrographs showing structural disorder are shown in Figs. 3 and 4. No significant changes in the appearance of this structural disorder could be seen by electron microscopy or by powder X-ray analysis of the preparations heated for a wide range of times, as different as 1 day or 4 weeks. We will refer to these structures as intergrowth tungsten bronzes.

The electron diffraction patterns of the intergrowth bronzes showed a characteristic streaking along $[100]$, as shown in Fig. 3c. The strong substructure reflections found in these patterns strongly resemble those of WO_3 itself. For more ordered regions within the crystals the streaking

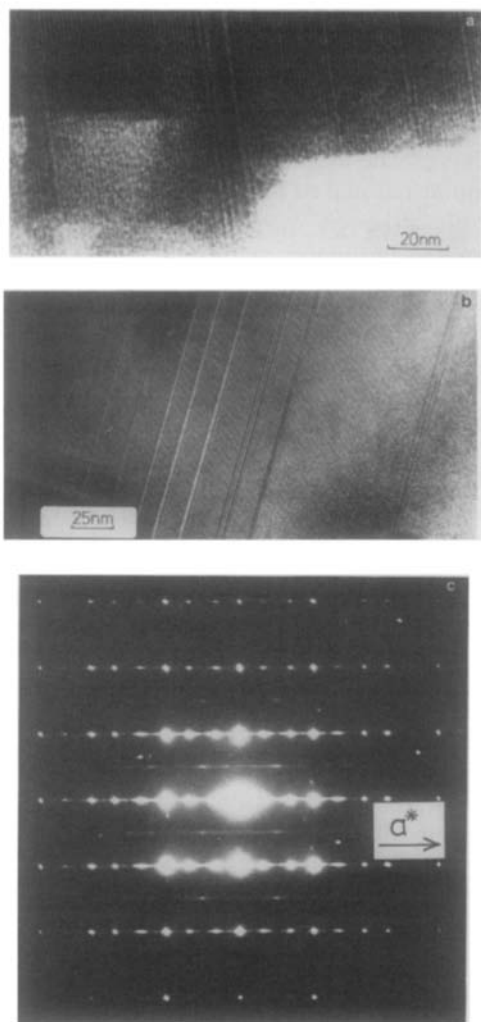


FIG. 3. (a, b, c.) Electron micrographs of different fragments of crystals from the intergrowth bronze region viewed along $[001]$. The disorder shown is typical of that found in these materials. (d) Diffraction pattern from a crystal fragment similar to those shown above. The prominent streaking is parallel to $[100]$ and was observed over the entire composition range $0.12 < x < 0.20$.

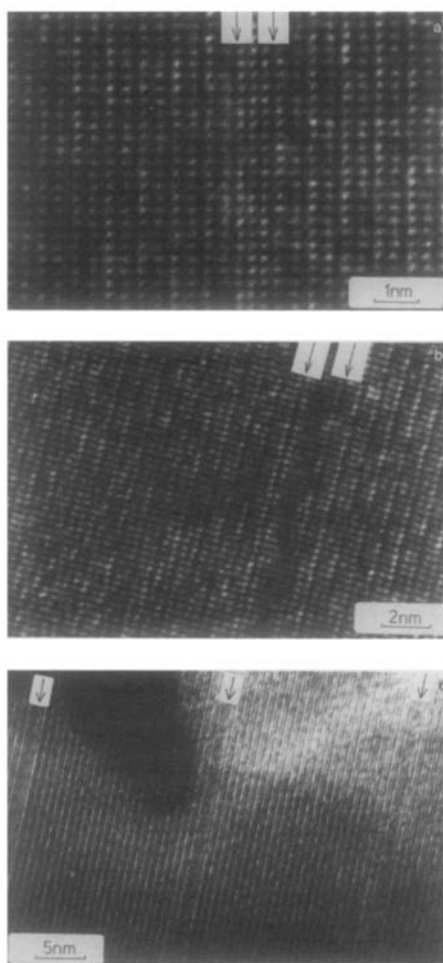


FIG. 4. High-magnification micrographs of crystals showing a variety of defect structures which are marked by arrows. (a) a slab of 3 WO_6 octahedra rows in a matrix consisting of double rows of octahedra. (b) a slab of 5 WO_6 octahedra in a matrix of double rows in a crystal of overall composition $\text{Sb}_{0.20}\text{WO}_3$. (c) a fragment of a crystal of overall composition $\text{Sb}_{0.18}\text{WO}_3$ showing a quasi-ordered repetition of the defects in (b) corresponding to $\bar{n} = 2.083$ and microcomposition $x = 0.194$.

along $[100]$ could be more or less distinguished as a number of distinct superstructure reflections between the WO_3 substructure reflections.

The high-resolution electron micrographs of the intergrowth bronzes showed that the major part of the structure consisted of

slabs of WO_3 -like structure, which were n octahedra in thickness. These WO_3 slabs were separated by fault planes or thin slabs of another structure type. As mentioned, it was found that in the crystals from preparations of higher antimony contents fairly large regions existed with an ordered intergrowth structure, which had $n = 2$ as shown in Fig. 4. No n values below 2 were ever observed and by lowering the antimony content the structural disorder increased and higher values of n were more frequently found. The highest n value observed in this study was 8, but a more detailed investigation using different preparation conditions, may show that higher n values can occur. It is notable that even numbers of n were much more frequently found than odd numbers.

Other Ternary Phases in the Region Close to WO_3

No other ternary phase was observed in this study in the region close to WO_3 , as has been indicated in the phase diagram in Fig. 1b. For instance, several samples were prepared at the overall compositions $Sb_{0.02}W_{0.98}O_{2.80}$ and $Sb_{0.02}WO_{2.80}$, as it has previously been reported that small amounts of many ternary metal ions initiate the formation of an oxide with the Mo_5O_{14} structure type (5) or an oxide close to $WO_{2.82}$ (6). For antimony, neither of these oxides was found. Preparations at $Sb_{0.02}W_{0.98}O_{2.72}$ and $Sb_{0.05}W_{0.95}O_{2.72}$ also revealed that no, or very little, antimony was substituted for tungsten in the $W_{18}O_{49}$ oxide, as other phases were found to be present besides the binary $W_{18}O_{49}$ oxide and no significant shifts were observed for the monoclinic unit-cell parameters of $W_{18}O_{49}$ found in these preparations compared with the binary oxide itself; typical values being $a = 1.833 \pm 1$ nm, $b = 0.3784 \pm 2$ nm, $c = 1.404 \pm 1$ nm, and $\beta = 115.2 \pm 1^\circ$. The X-ray results themselves do not, of course, rule out the possibility that a small

amount of antimony is substituting into this oxide, and as we have not made any chemical analysis of the products this point must be left open here.

Interpretation of the Intergrowth Bronze Structure

Although we are aware that a visual comparison of an electron micrograph with a structural model may give rise to errors of interpretation if no computer calculated images are used, they give at least a qualitative picture. In our case, however, we have already some structural information from the earlier single-crystal X-ray data from a crystal of composition $Sb_{0.15}WO_3$. About 800 reflections were used from Weissenberg photographs and by the Patterson technique a heavy-atom model was constructed. This gave the suggested structures shown in Fig. 5b. A comparison with the electron micrograph in Fig. 5a shows very good agreement between this structural model and the contrast from the ordered regions within the crystals, where $n = 2$.

Assuming that this interpretation of the ordered structure is correct, it leads to the conclusion that the observed fault planes in the intergrowth bronze can be looked upon as very thin slabs of the hexagonal tungsten bronze (HTB) structure. These slabs are only one hexagonal tunnel thick. The antimony intergrowth tungsten bronzes belong therefore to the family of intergrowth tungsten bronzes (ITB) previously reported by Hussain and Kihlberg for a number of M_xWO_3 systems (7).

This structural interpretation allows us to calculate the exact chemical microcomposition of a crystal by a statistical study of the n values which occur. As an example, a region of a disordered crystal is shown in Fig. 6a. The observed n values and their related frequencies have been recorded in Fig. 6b. In this case the mean value of n was found to be 2.125. In Fig. 6b we can see that we have a clear maximum for the value

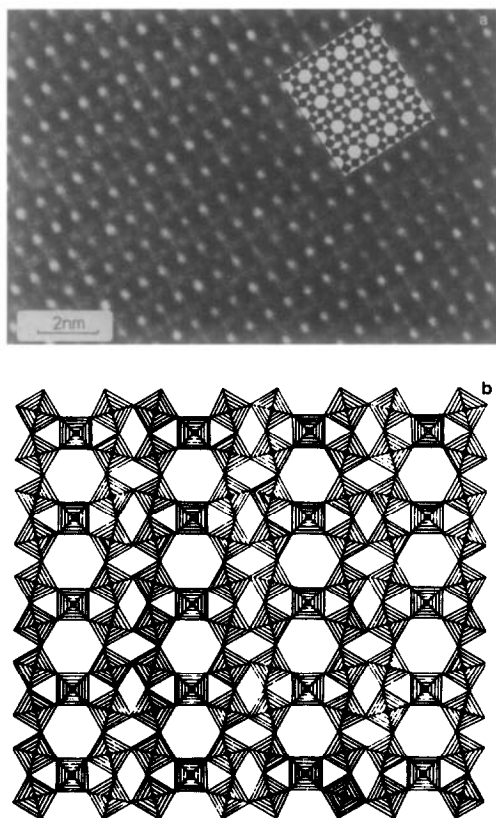


FIG. 5. (a) High-resolution electron micrograph of an ordered part of a crystal from a sample of overall composition $\text{Sb}_{0.20}\text{WO}_3$ viewed along [001]. (b) Proposed structure of the ordered $\text{Sb}_{0.20}\text{WO}_3$ phase deduced from X-ray diffraction. The structure here is in good agreement with the image in (a), as can be seen by the superimposed structural drawing in (a).

2, which is not surprising in view of the fact that the crystal contains rather large regions of the ordered $n = 2$ structure. In the histogram we can also see that even n values are favored. Knowing the mean n value, we can now calculate the average composition for the area studied by the formula $x = 1/(2n + 1)$, which in the chosen example gives $x = 0.19$, or $\text{Sb}_{0.19}\text{WO}_3$. We must, however, stress the point that in the use of this formula we assume that every hexagonal tunnel is fully occupied with Sb atoms or ions. If the average occupancy is lower, the average x value will be lowered

in a proportional way. In the study of a large number of crystals from preparations of different gross compositions, we have certainly found a spread in the calculated x values between different crystals of the same preparation, but no significant trends in the average of the calculated x values compared with overall composition which would indicate a more significant deviation from full or nearly full occupancy of the tunnels.

The totally ordered ITB structure with $n = 2$ would, in this way, be given the composition $\text{Sb}_{0.20}\text{WO}_3$, which is in agreement with the findings of the powder X-ray analysis. However, we have not found one macroscopic well-ordered single crystal, even by examination of crystals from preparations of overall compositions of $\text{Sb}_{0.20}\text{WO}_3$ or higher, and in all preparations, in spite of long heating times, electron microscopy always revealed some structural disorder. This explains the

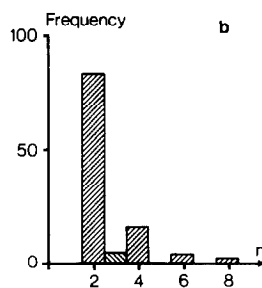
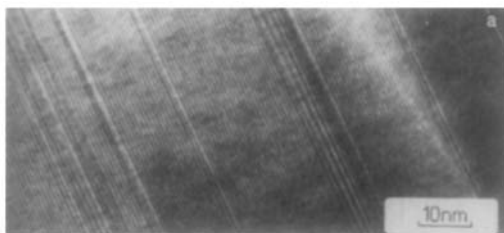


FIG. 6. (a) Low-magnification electron micrograph of a disordered Sb_xWO_3 crystal. (b) Histogram showing the distribution of n values over a large region of the crystal shown in (a). The mean n value, \bar{n} , was found to be 2.125 corresponding to a microcomposition of $x = 0.19$ in Sb_xWO_3 .

difficulties encountered in the earlier attempts to refine the structural model from the single-crystal X-ray data.

Discussion

It was found, both for the perovskite-related and for the intergrowth bronzes, that varying the heating time from 1 day up to 2 months had no significant effect upon the reaction products. The first conclusion to be drawn from this fact must be that the initial reaction proceeds rapidly and, secondly, once formed these phases undergo no, or very small, changes with times. This is notable in the case of the ITB phases, which evidently are rather disordered.

A comparison of the Sb_xWO_3 system with other M_xWO_3 systems where intergrowth bronzes have been found is of some interest. First of all, we can consider the ITB structures found to form with K, Rb, Cs, and Tl (7). All these structures can be regarded as an intergrowth of HTB and WO_3 slabs, in a similar way as now found for antimony. These structures differ, however, in that the most frequently occurring thickness of the HTB structure slabs consists of two rows of hexagonal tunnels. The compositional range for the alkali metal double-tunnel ITB structures, as determined by phase analysis, was found to be $0.06 < x < 0.10$ and preparations always resulted in mixtures of several ITB structures (8, 9). This inhomogeneity behavior parallels the antimony ITB structures to some extent and it is interesting to note that the phase range for antimony is exactly twice that above, being $0.12 < x < 0.20$. However, in the case of antimony, by assuming full occupancy of the hexagonal tunnels, we have a rather ordered structure at $Sb_{0.2}WO_3$. A similar observed structure at $M_{0.1}WO_3$ in the alkali bronzes has not been observed.

A series of intergrowth bronzes also form in the Sn_xWO_3 system (10). For high Sn

contents the ITB structures resemble those found for the alkali metals, with HTB slabs of double tunnel thickness separated by WO_3 slabs. The thickness of the WO_3 slabs seem to be fairly well ordered when they consist of only two or three octahedra. At lower Sn contents towards $x = 0.05$ another type of intergrowth bronze is found with so far an unknown structure. A series of intergrowth bronzes very similar to those in the tin system, have also been reported for Pb_xWO_3 (11) and Ba_xWO_3 (12). In the barium system in particular, a well-ordered bronze structure occurs at about $x = 0.15$. The actual structure of this barium phase has yet not been solved, but the results gained in the Sb_xWO_3 and Sn_xWO_3 systems suggest that some type of ITB structure is likely.

A number of ternary elements are now known to form intergrowth tungsten bronzes. A feature that all these elements have in common is that the size of the ternary ion to be found in the bronze is fairly large (12). It is an experimentally found rule that in tungsten bronzes the valence of the ternary ion has the lowest possible value, and so in this case the ternary ion must be considered to be Sb^{3+} . A list of empirical effective ion radii for these elements in octahedral coordination, gives values in the range 0.12–0.17 mm (13). A similar value for comparison of the Sb^{3+} ion is not given, but an extrapolation from the table would suggest a value of the order of 0.09 mm. At a first sight this seems to fall outside the general trend observed for the other elements. However, the Sb^{3+} ion has a lone electron pair and it is a general experience that such an ion often exhibits irregular coordination which does not result in consistent interatomic distances. The actual size to consider in the case of the Sb^{3+} ion is certainly much larger than that indicated above and may well fall into the above range, being >0.12 mm (14).

The two group IVB members Sn and Pb

in the periodic table form ITB structures as does the group VB member Sb, as reported here. From this point of view, the bigger Bi^{3+} ion of the same VB group would be expected to be another metal that formed ITB phases. No such structures have been found in the previously published analysis by one of us (2). It is therefore possible that the synthesis must be made under high pressure. An investigation of such samples by electron microscopy would be of great interest.

Acknowledgments

M.P. is grateful to Professor Bijl for extending his hospitality during study leave at the University of Bradford, where the present work was carried out. R.J.D.T. is indebted to the Science Research Council, London, for an equipment grant. This study has also partly been performed within a research program supported by the Swedish Natural Science Research Council (T.E.).

References

1. M. PARMENTIER, C. GLEITZER, AND A. COURTOIS, *Mater. Res. Bull.* **10**, 341 (1975).
2. M. PARMENTIER AND C. GLEITZER, *C.R. Acad. Sci. Sér C* **281**, 819 (1975).
3. T. EKSTRÖM AND R. J. D. TILLEY, *Mater. Res. Bull.* **9**, 705 (1974).
4. R. J. D. TILLEY AND J. R. GANNON, *J. Microsc.* **106**, 59 (1976).
5. T. EKSTRÖM AND R. J. D. TILLEY, *J. Solid State Chem.* **19**, 125 (1976).
6. R. PICKERING AND R. D. J. TILLEY, *J. Solid State Chem.* **16**, 247 (1976).
7. A. HUSSAIN AND L. KIHNBORG, *Acta Crystallogr. Sect. A* **32**, 551 (1976).
8. A. HUSSAIN, *Acta Chem. Scand. A* **32**, 479 (1978).
9. A. HUSSAIN, *Chem. Commun. Univ. Stockholm*, No. 2 (1978).
10. R. STEADMAN, R. J. D. TILLEY, AND I. J. MCCOLM, *J. Solid State Chem.* **4**, 199 (1972).
11. T. EKSTRÖM AND R. J. D. TILLEY, *J. Solid State Chem.* **24**, 209 (1978).
12. T. EKSTRÖM AND R. J. D. TILLEY, *J. Solid State Chem.* **28**, 259 (1979).
13. R. D. SHANNON AND C. T. PREWITT, *Acta Crystallogr. Sect. B* **25**, 925 (1969).
14. J. GALY, G. MEUNIER, S. ANDERSSON, AND A. ÅSTRÖM, *J. Solid State Chem.* **13**, 142 (1975).